Virologica Sinica 39 (2024) 537–545

Contents lists available at ScienceDirect

Virologica Sinica

journal homepage: www.keaipublishing.com/en/journals/virologica-sinica
www.virosin.org

Research Article

RNA viromes of *Dermacentor nuttalli* ticks reveal a novel uukuvirus in Qīnghǎi Province, China

Yaohui Fang [a,b], Jun Wang [a], Jianqing Sun [c], Zhengyuan Su [a], Shengyao Chen [a,b], Jian Xiao [a,b], Jun Ni [a,b], Zhihong Hu [a], Yubang He [c], Shu Shen [a,d,e,*], Fei Deng [a,*]

[a] *Key Laboratory of Special Pathogens and Biosafety and National Virus Resource Center, Wuhan Institute of Virology, Chinese Academy of Sciences, Wuhan 430071, China*
[b] *University of Chinese Academy of Sciences, Beijing 101408, China*
[c] *Qīnghǎi Lake National Nature Reserve Administration, Xining 810000, China*
[d] *Hubei Jiangxia Laboratory, Wuhan 430200, China*
[e] *Xinjiang Key Laboratory of Vector-borne Infectious Diseases, Urumqi, 830002, China*

ARTICLE INFO

Keywords:
Dermacentor nuttalli
Qīnghǎi Province
Virome
Uukuvirus
M segment

ABSTRACT

Ticks are a major parasite on the Qīnghǎi-Tibet Plateau, western China, and represent an economic burden to agriculture and animal husbandry. Despite research on tick-borne pathogens that threaten humans and animals, the viromes of dominant tick species in this area remain unknown. In this study, we collected *Dermacentor nuttalli* ticks near Qīnghǎi Lake and identified 13 viruses belonging to at least six families through metagenomic sequencing. Four viruses were of high abundance in pools, including Xīnjiāng tick-associated virus 1 (XJTAV1), and three novel viruses: Qīnghǎi Lake virus 1, Qīnghǎi Lake virus 2 (QHLV1, and QHLV2, unclassified), and Qīnghǎi Lake virus 3 (QHLV3, genus *Uukuvirus* of family *Phenuiviridae* in order *Bunyavirales*), which lacks the M segment. The minimum infection rates of the four viruses in the tick groups were 8.2%, 49.5%, 6.2%, and 24.7%, respectively, suggesting the prevalence of these viruses in *D. nuttalli* ticks. A putative M segment of QHLV3 was identified from the next-generation sequencing data and further characterized for its signal peptide cleavage site, N-glycosylation, and transmembrane region. Furthermore, we probed the L, M, and S segments of other viruses from sequencing data of other tick pools by using the putative M segment sequence of QHLV3. By revealing the viromes of D. nuttalli ticks, this study enhances our understanding of tick-borne viral communities in highland regions. The putative M segment identified in a novel uukuvirus suggests that previously identified uukuviruses without M segments should have had the same genome organization as typical bunyaviruses. These findings will facilitate virus discovery and our understanding of the phylogeny of tick-borne uukuviruses.

1. Introduction

Ticks are blood-sucking parasites of animals and important vectors for a variety of pathogens associated with zoonotic diseases (Boulanger et al., 2019). Over 100 different species of ticks are widely distributed across China, with 27 species having an economic impact on agriculture and animal husbandry in parts of the Qīnghǎi-Tibet Plateau, including Qīnghǎi Province and the Tibet Autonomous Region located in western China (Yang et al., 2008). In Qīnghǎi, tick species of the genera *Argas*, *Dermacentor*, *Haemaphysalis*, *Ixodes*, and *Rhipicephalus* occur in different locations. Nine species inhabit the northern mountainous area, eight species inhabit the central basin, and 19 species inhabit the southern plateau (Yang et al., 2008).

A variety of pathogenic bacteria and parasites have been identified in ticks in Qīnghǎi, such as tick-borne rickettsioses, *Borrelia burgdorferi, Babesia abigemina*, and Theileria species, which cause fatal tick-borne spotted fever and Lyme disease in humans, as well as bovine babesiosis and Taylor's disease in cattle and sheep (Han et al., 2018; Geng et al., 2010; Li Y. et al., 2015; Yin et al., 2004). Therefore, tick-borne pathogens pose a threat to public health and can lead to significant economic losses in the livestock industry (Yu et al., 2015). Qīnghǎi Province is a potential natural foci of the highly pathogenic tick-borne virus, Crimean-Congo

* Corresponding authors.
E-mail addresses: df@wh.iov.cn (F. Deng), shenshu@wh.iov.cn (S. Shen).

https://doi.org/10.1016/j.virs.2024.04.006
Received 17 December 2023; Accepted 23 April 2024
Available online 26 April 2024

hemorrhagic fever virus (CCHFV), because the antibody response to this virus has been detected in humans, livestock, rodents, and birds (Zhao et al., 2012). However, neither CCHFV itself, nor human cases of CCHFV infection, have been isolated or confirmed from any of these samples (Zhao et al., 2012). Recently, a new subtype (Himalayan) of Eastern tick-borne encephalitis virus (TBEV) was identified in wild Himalayan marmots (*Marmota himalayana* (Hodgson, 1841)) in the Qīnghǎi-Tibet Plateau (Dai X. et al., 2018). However, the prevalence of this virus among wild and domestic animals and tick vectors, as well as the public health significance, remains unclear. To date, few studies have reported the viromes of ticks on the Qīnghǎi-Tibet Plateau. Therefore, as it remains unclear whether ticks in Qīnghǎi can carry viruses such as TBEV, CCHFV, or any other viral pathogens, research must be conducted on tick viromes to identify potential tick-borne viral pathogens. Such research has benefits for treating emerging diseases associated with tick-borne viruses.

In this study, we investigated the viromes of *Dermacentor nuttalli* ticks collected from grazing animals in Qīnghǎi using next-generation sequencing (NGS). We then analyzed the sequences of novel viruses and their prevalence among tick groups. From the sequencing data, we identified a putative M segment of the novel uukuvirus and characterized its potential as a viral glycoprotein (GP). These results improve our understanding of the viromes of *D. nuttalli* ticks in highland regions. Moreover, identification of the putative M segment sequence of the novel uukuvirus suggests the essential role of the structural envelope GP in constructing segmented bunyaviruses. The method used to search for this M segment may help further studies in discovering novel segmented viruses containing envelope GPs, which differ from related known viruses.

2. Materials and methods

2.1. Sampling of ticks

From 2015 to 2017, 3,162 ticks were collected from cattle, sheep, and goats at three locations near Qīnghǎi Lake in Qīnghǎi Province, China. These ticks were identified as *D. nuttalli* according to their morphology (Deng, 1978). All samples were captured alive and stored at −80 °C until further processing. The ticks were divided into groups according to the sampling location and time (Supplementary Table S1).

2.2. Determining tick species using internal transcribed spacer 2 (ITS2) sequences

Ticks were washed three times using pre-cooled sterile phosphate-buffered saline buffer (PBS, 0.01 M, PH = 7.2−7.6) (Boster Bio, Hong-Kong, China), then homogenized in 500 μL of PBS using Tissue Cell-Destroyer (NewZongKe, Wuhan, China). Then centrifuging at 2,500×*g*, 4 °C for 5 min. The total DNA was purified from the clarified tick homogenates (300 μL) using the Pure Link™ Genomic DNA Mini Kit (Life Technologies, Carlsbad, USA). Tick ITS2 rDNA were amplified using primers TITS2F1 (5′-CGAGACTTGGTGTGAATTGCA-3′) and TITS2R1 (5′-TCCCATACACCACATTTCCCG-3′) (Chitimia et al., 2009; Lu et al., 2013). PCR reactions were performed in 50 μL volumes containing 2 μL DNA (100 ng), 2 μL of each primer (20 μmol/L) and 25 μL 2 × High-Fidelity Master Mix (Tsingke, Beijing, China) under the following conditions: 95 °C for 5 min (initial denaturation) followed by 30 cycles of 95 °C for 15 s (denaturation), 57 °C for 15 s (annealing), and 72 °C for 30 s (extension), with a final extension of 72 °C for 5 min. PCR product sequences (1350 bp) were analyzed by Sanger sequencing and used to characterize the tick phylogeny.

2.3. Next-generation sequencing

After homogenizing the tick sample, centrifuging at 2,500×*g*, 4 °C for 5 min, 300 μL of supernatant was mixed with 700 μL TRI Reagent® (Merck, Darmstadt, Germany), left to stand for 5 min. Then, a vortex stirrer was used after adding 400 μL of chloroform (Sinopharm, Beijing, China), which was centrifuged at 12,000×*g*, 4 °C for 15 min. The supernatant was mixed with 500 μL of isopropanol (Sinopharm), kept at −80 °C for 30 min, and centrifuged at 12,000×*g*, 4 °C for 15 min. Finally, the supernatant was discarded, and the mixture washed twice with 70% ethanol (Sinopharm), before dissolving the precipitate in diethylpyrocarbonate-treated water (Beyotime, Shanghai, China) at 55 °C. All RNA solutions were then pooled in equal quantity and quality and checked using an Agilent 2100 Bioanalyzer (Agilent Technologies, Santa Clara, USA). The TrueSeq Total RNA Library Preparation Protocol (Illumina, San Diego, USA) were used for library construction. rRNA was removed using the Ribo-Zero-Gold (Human-Mouse-Rat) kit (Illumina). Pair-end (150 bp) sequencing of each library was performed using a HiSeq 3000 platform (Illumina).

2.4. Sequence assembly and RNA virus discovery

For each library, the raw read quality was first evaluated using FastQC (version 0.11.5). Trimmomatic program (version 0.32) was used to reject low-quality sequences (LEADING: 20, TRAILING: 20, MINLEN: 36) (Bolger et al., 2014). The non-filtering host clean reads were assembled de novo using the Trinity program (version 2.1.1) with default parameter settings (Grabherr et al., 2011). The assembled contigs were first compared (using BLASTX and BLASTN) against a database of all reference viral nucleotides (vnt) and viral proteins (vaa) (NCBI, virus taxid:10239). All contig-matched viral databases were extracted for comparison (using BLASTN and BLASTX) against the databases of all reference nucleotides (nt) and proteins (nr) (NCBI, Nucleotide collection). To obtain more credible results, we set the e-value to 0.00001. Megan5 (version 5.11.3) was used to view the BLAST output file (.xml) and extracted virus contigs (Huson et al., 2007). The virus classification and nomenclature are referenced from ICTV (International Committee on Taxonomy of Viruses) (Kuhn et al., 2023). Some contigs still showed homology after Trinity assembly; these were subsequently assembled using SeqMan (DNAstar Inc., Madison, USA) with default parameter settings. Bowtie2 (version 2.3.1) was used to calculate the read number of each contig and assess its abundance (Langmead and Salzberg, 2012). The calculation of TPM (transcript per million) for gene i uses the following formula (Zhao et al., 2021):

$$TPM_i = \frac{q_i / l_i}{\sum_j (q_j / l_j)}$$

where q_i denotes reads mapped to transcript, l_i is the transcript length, and $\sum_j (q_j / l_j)$ corresponds to the sum of mapped reads to transcript normalized by transcript length.

2.5. Phylogenetic and sequence analyses

For phylogenetic analysis, all assembled sequences were aligned with reference sequences using ClustalW with default parameter settings. Phylogenetic relationships were estimated using the maximum likelihood method with 1000 replications in the bootstrap test. Maximum likelihood analyses were performed using MEGA6 (Version 6.06) (Tamura et al., 2013). The Conserved Domain Database was also used to identify the conserved domain of the virus and perform conserved domain annotation of the new virus (https://www.ncbi.nlm.nih.gov/Structure/cdd/wrpsb.cgi/). EditSeq and MegAlign software (DNAstar Inc.) were used to analyze the basic characteristics of the sequences, providing assessments of parameters such as molecular weight, GC content, and sequence identity. The prediction of N-glycosylation modification sites was conducted using NetNGlyc 1.0 Server (http://www.cbs.dtu.dk/services/NetNGlyc/), transmembrane region prediction was performed using TMHMM Server 2.0 (http://www.cbs.dtu.dk/services/TMHMM/), and signal peptide cleavage sites were identified using SignalP 4.0 (http://www.cbs.dtu.dk/services/SignalP/).

2.6. Assays to detect the cleavage and N-glycosylation of the putative viral glycoprotein

Following a previous study (Dai S. et al., 2018), a recombinant baculovirus carrying Qīnghǎi Lake virus 3 glycoprotein (QHLV3 GP), fused with a Strep-tag at the N-terminus and a Flag-tag at the C-terminus, was constructed using the pFastBac™ Dual vector (Invitrogen, Carlsbad, USA). The Sf9 cells were treated with 10 μg/mL tunicamycin (abcam, Cambridge, UK) or Dimethyl sulfoxide (DMSO) (Merck) as control, then infected with the recombinant baculovirus at a multiplicity of infection of one. The lysates were collected at 72 h post infection and Western blot assays were performed as described in a previous study (Dai S. et al., 2018).

2.7. Molecular epidemiological surveys of viruses in tick groups

For the viral epidemiological investigation, RNA was extracted in the same manner as that for library construction. Then, at least 10 μg of RNA was used to reverse the transcription reaction, which was performed in 50-μL volumes. First, RNA were mixed with 1 μL of random primer after incubating at 70 °C for 5 min then placing immediately on ice for 2 min. The RNA were then mixed with 1 μL dNTP, 1 μL M-MLV Reverse Transcriptase (Promega, Madison, USA), and 1 μL RNase Inhibitor (Promega) under the following conditions: 25 °C, 10 min; 37 °C, 60 min; 75 °C, 15 min. Nested PCR were used to detected the RNA viruses, and PCR reaction were performed in 50-μL volumes, including 2 μL cDNA, 2 μL of each 20 μmol/L primer, and 25 μL 2 × High-Fidelity Master Mix (Tsingke) under the following conditions: 95 °C for 5 min (initial denaturation); followed by 35 cycles of 95 °C for 15 s (denaturation); 56 °C for 15 s (annealing); 72 °C for 15 s (extension); and a final extension of 72 °C for 5 min. PCR products were used as templates with nested primers to perform a second round of amplification under the same conditions. All primers used in this study are described in Supplementary Table S2.

2.8. Statistical analyses

Statistical analyses were performed using GraphPad Prism, version 8 (GraphPad Software). The statistical significance of differences between two groups was analyzed using Student's *t*-test, and the kappa test was used to analyze the relationship between L, S, and M segments. Statistical significance was set to $P < 0.05$. The Cohen's κ-coefficient was used as a metric of interrater agreement (Xia, 2020).

3. Results

3.1. Novel virus sequences identified from the viromes of D. nuttalli ticks in Qīnghǎi

Between 2015 and 2017, 3162 ticks were collected from cattle around Qīnghǎi Lake in Qīnghǎi Province, China. These ticks were identified as *D. nuttalli* by morphological examination, which was verified by phylogenetic analysis of partial ITS2 sequences (Supplementary Fig. S1). The ticks were divided into 97 groups (n = 17–336 per group) according to the sampling time, sampling site, and feeding status (Supplementary Table S1).

Six tick pools (one pool in 2015, two pools in 2016, and three pools in 2017) were prepared by mixing equivalent amounts of total RNA purified from two to three randomly selected tick groups, then subjected to NGS, which generated 21,959,458–122,540,082 total reads (Supplementary Table S1). Despite the limited abundance compared with the large number of reads related to eukaryotes, virus-related reads were found in all six pools, ranging from 10 to 11,003, accounting for 0.000013–0.1% of the total reads (Fig. 1A, Supplementary Table S1). Viromes of *D. nuttalli* ticks were characterized by merging the two pools from 2016 and three pools from 2017 (Fig. 1B, Supplementary Fig. S2). Viral sequences were predominantly found in six different families: *Phenuiviridae*, *Nairoviridae*, *Rhabdoviridae*, *Toitiviridae*, *Sedoreoviridae*, and *Hepeviridae*. We also identified sequences related to unclassified viruses and those belonging to realm *Riboviria* but could not be assigned to any other genus (Fig. 1B).

Virus-related sequences with reference to Chāngpíng tick virus 1, belonging to family *Phenuiviridae*, and three unclassified viruses, including Hepeviridae sp., Ixodes scapularis associated virus 3, and Xīnjiāng tick-associated virus 1 (XJTAV1), were found in high abundance [transcripts per million (TPM) > 0.1] compared with other viruses. The sequences related to XJTAV1 had high amino acid identity (99%) to the reference sequence, suggesting that it is a new strain of this virus and designated as strain QH-2015. The other three viruses were of comparatively low identities to the reference viruses by comparing their amino acid sequences, suggesting that these are novel viruses, and thus they are named as Qīnghǎi Lake virus 1 (QHLV1), Qīnghǎi Lake virus 2 (QHLV2) and Qīnghǎi Lake virus 3 (QHLV3) (Table 1).

3.1.1. Xīnjiāng tick-associated virus 1

The XJATV1 sequence was found in library 2015-1 (2641 nt in length) and contained two open reading frames (ORFs). This new XJATV1 strain shared high nucleotide and amino acid sequence

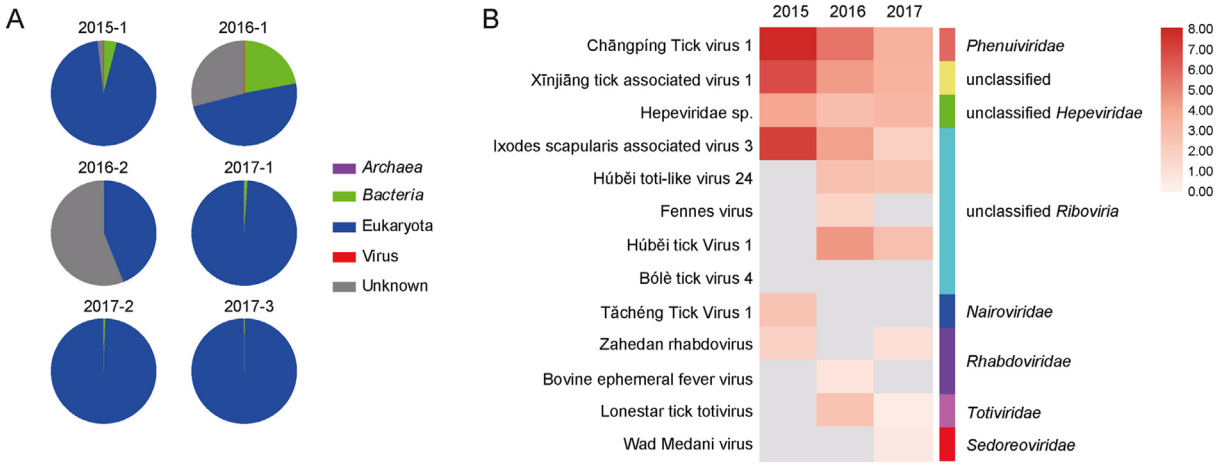

Fig. 1. Viral abundance of *Dermacentor nuttalli* ticks according to metagenomics analysis. **A** Proportions of the numbers of reads assigned to eukaryotes, bacteria, and viruses, and number of unassigned reads in each of the six pools shown as pie charts. **B** Heatmap of the TPM of viruses identified from 2015 to 2017. TPM, transcripts per million.

Table 1
Viruses identified from *D. nuttalli* tick pools by RNA-seq.

Provisional virus name	Segment	Length (bp)	Reference (amino acid identity)	Virus family	TPM	Accession number
Xīnjiāng tick associated virus 1		2641	Xīnjiāng tick associated virus 1 (99%)	Unclassified	106.77	OR911991
Qīnghǎi Lake virus 1		5465	*Hepeviridae* sp. (71%)	Unclassified	14.62	OR911992
Qīnghǎi Lake virus 2		1496	*Ixodes scapularis* associated virus 3 (68%)	Unclassified	142.61	OR911993
Qīnghǎi Lake virus 3	L	6655	Chāngpíng tick virus 1, L segment (83%)	*Phenuiviridae*	3.36	OR837771
	M	3397	None	*Phenuiviridae*	3.30	OR837773
	S	1894	Chāngpíng tick virus 1, S segment (77%)	*Phenuiviridae*	1.60	OR837772

similarities (96% and 99%, respectively) with the reference virus (MH688544) and had a similar genome organization to the Medway virus, which belongs to the genus *Sobemovirus*. ORF1 [511 amino acids (aa)] encodes a protease containing a trypsin-like peptidase domain (167–276 aa) and ORF2 (244 aa) encodes an RNA-directed RNA polymerase (RdRp) containing an RT-like superfamily (7–156 aa) (Supplementary Fig. S3).

3.1.2. Qīnghǎi Lake virus 1

The QHLV1 sequence was 5465 nt in length and contained one ORF encoding RdRp (1797 aa). This sequence is related to an unclassified positive-stranded RNA virus of family *Hepeviridae*, *Hepeviridae* sp. (MZ244288), recovered from a bird anal swab in a metagenomic study (Tokarz et al., 2014). Three conserved domains were found: the RNA methyltransferase domain (38–347 aa), RNA helicase (608–849 aa), and the RdRp domain (1005–1375 aa) (Supplementary Fig. S3). Viruses of genus *Omegatetravirus* usually contain two segments: RNA1 (approximately 5.3 kb), which encodes an RdRp, including the three aforementioned domains, and RNA2 (approximately 2.5 kb), which encodes a capsid protein. QHLV1 showed a similar genome organization to the RNA1 segment of omegatetraviruses (Supplementary Fig. S3).

3.1.3. Qīnghǎi Lake virus 2

QHLV2 was 1496 nt in length and contained one ORF encoding a 396-aa hypothetical protein (Supplementary Fig. S3). This hypothetical protein shared low identity (33% for nucleotides and 68% for protein

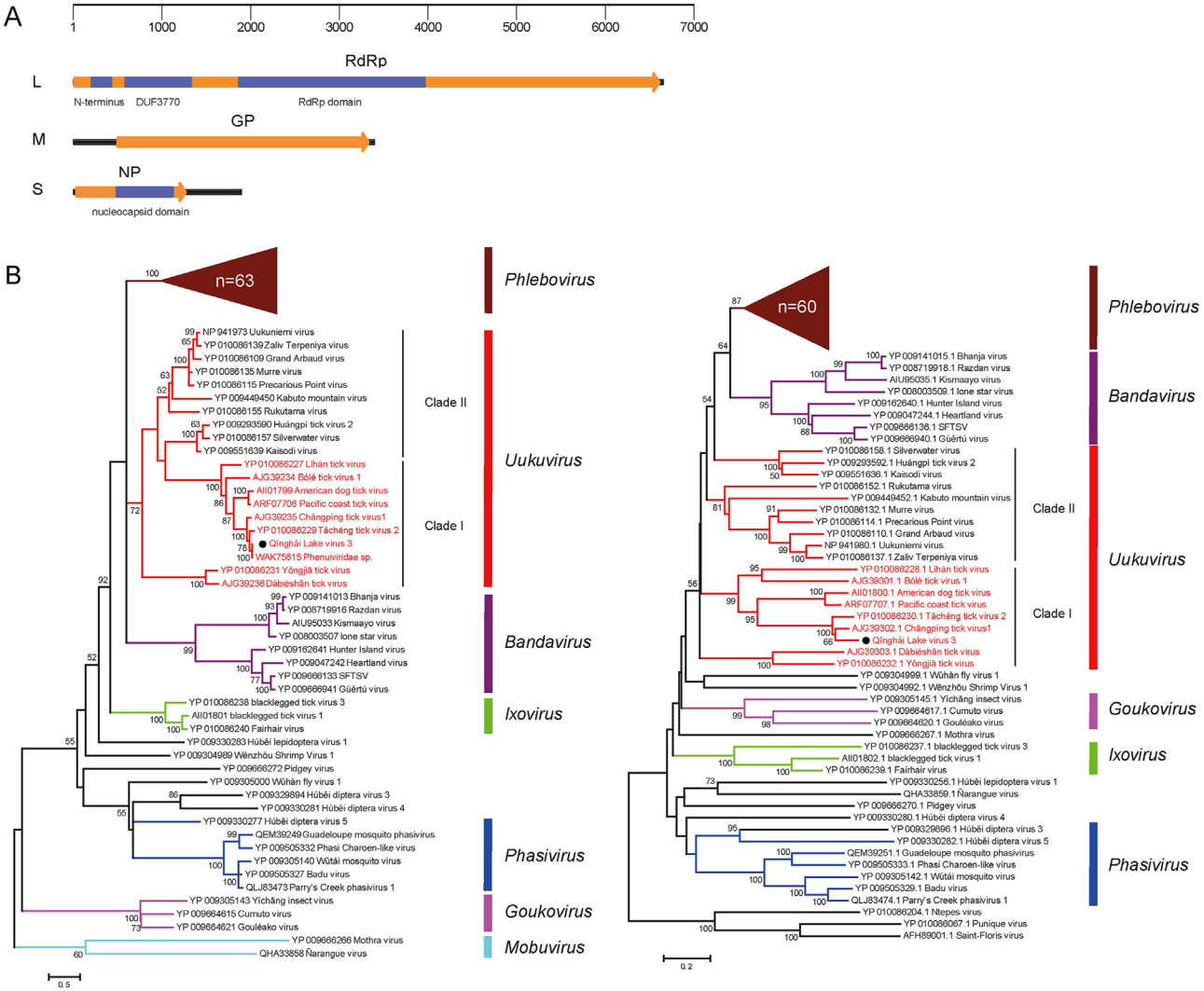

Fig. 2. Phylogenetic relationships and genome organizations of QHLV3. **A** Genome organizations of QHLV3. Black lines represent contigs, yellow arrows represent ORFs, and purple regions represent conserved domains. **B** Phylogenetic trees of QHLV3 L and S segments. Red font indicates the uukuvirus lacking the M segment. QHLV3, Qīnghǎi Lake virus 3; ORF, open reading frame.

sequence) with the capsid protein of the Drosophila A virus identified in *Drosophila melanogaster*, which contains two ORFs encoding RdRp and a capsid protein (Ambrose et al., 2009). Therefore, this 1496-nt sequence may be a partial genome sequence of QHLV2 (Supplementary Fig. S3, Table 1).

3.1.4. *Qīnghǎi Lake virus 3*

QHLV3 sequences were found in five of the six tick pools by RNA-seq (Supplementary Table S3); however, only the L and S segments were identified by BLAST analyses. This was similar to the reference virus, Chāngpíng tick virus 1, which is a novel uukuvirus previously identified in ticks in Běijīng, China, but without the M segment that should be present in uukuviruses such as Uukuniemi virus (Shi et al., 2016). Taking the QHLV3 sequences found in the pool 2017-1 for example (Supplementary Table S3), the L segment of this virus was 6655 nt in length and encoded RdRp (2198 aa) containing an endonuclease domain (65–137 aa), a DUF3770 super family (193–436 aa), and an RdRp domain (621–1315 aa) (Fig. 2A), and its S segment was 1894 nt in length and encoded the nucleocapsid protein (Fig. 2A). Phylogenetic trees of the L and S segments showed that QHLV3 was clustered with the Chāngpíng tick virus1, Tǎchéng tick virus 2 (TcTV2), American dog tick virus (ADAV), Pacific coast tick virus (PACV), Lǐhán tick virus (LITV), Bólè tick virus 1, Dàbiéshān tick virus (DBTV), Yǒngjiā tick virus (YONV), and *Phenuiviridae* sp. to form clade I, all of which lacked the M segment, whereas the other uukuviruses containing M segments formed clade II (Fig. 2B).

3.2. *Identification and characterization of a putative M segment of QHLV3*

QHLV3 would have a similar abundance in each segment in the RNA-seq pools. If an M segment existed for this virus, it would have a comparable TPM value to that of the L and S segments. Uukuviruses generally have an ORF coding for a GP of 900–1500 amino acids in length. Therefore, we searched for a putative M segment from the unassigned contig sequences from the five QHLV3 positive pools based on the following conditions: 1) the theoretical abundance of putative M segment should be around the TPM values of QHLV3 L and S segments; 2) the theoretical length of the putative M segment should be 2000–5000 nt; and 3) the putative M segment should encode an ORF of 900–1500 aa in length. As a result, we identified one contig sequence, which was 3397 nt in length with a TPM value of 3.30 comparable to that of the QHLV3 S and L segments, from the pool 2017-1 (Table 1, Supplementary Table S3). Similar to the M segment of other uukuviruses from clade II, which are of 3229–3568 nt in length and encode envelope GPs of 1008–1012 aa, this putative M segment contained an ORF of 2929 nt encoding a protein of 943 aa (Fig. 2A). Sequences of this putative M segment were also identified in the other four tick pools, from which the QHLV3 S and L segment sequences were found (Supplementary Table S3). Generally, in the three pools of 2015-1, 2017-2, and 2017-3, the sequences of M segment (3339–3397 nt in length) all contained one ORF encoding a hypothetical protein of 943 aa, which was of high identity (99.1–99.6%) with the ORF sequence encoded by that found in pool 2017-1. Probably due to the inadequate sequencing depth of pool 2016-1, similar to the partial sequences of L and S segments, partial sequence of the putative M segment was identified.

The GPs of uukuviruses, phleboviruses, and bandaviruses typically contain one to three transmembrane domains and one to two signal peptides. Similarly, the protein encoded by the putative M segment was predicted to have two N-glycosylation sites (N453 and N852), two transmembrane domains (N347–N369; N382–N404), and two signal peptide sites (N101; N397) (Fig. 3A), despite QHLV3 GP having only 8.2–10.6% identity with the other proteins (Supplementary Fig. S4). Among all characterized uukuviruses, phleboviruses, and bandaviruses, the position of the cleavage site (N397) was highly conserved right after the second signal peptide, which, like the other uukuviruses, phleboviruses, and bandaviruses, generated the Gn and Gc fragments from the GP (Fig. 3A and B).

Glycosylation and cleavage of the QHLV3 GP were further confirmed by western blotting using a baculovirus expression system (Fig. 3C). QHLV3 Gn (~33 kDa) expression was detected in AcMNPV-GP-infected Sf9 cells at an identical position to that in cells treated with tunicamycin, an inhibitor of N-glycosylation, suggesting that QHLV3 Gn was not glycosylated. With tunicamycin treatment, the Gc (~60 kDa) was blotted in a lower position comparing with that without tunicamycin treatment, suggesting this putative viral protein has N-glycosylation. Uncleaved GP (~104 kDa) was also detected when blotting Gn with tunicamycin treatment. It is suggested that N-glycosylation is important for GP cleavage, and that GP cleavage could be inhibited when N-glycosylation

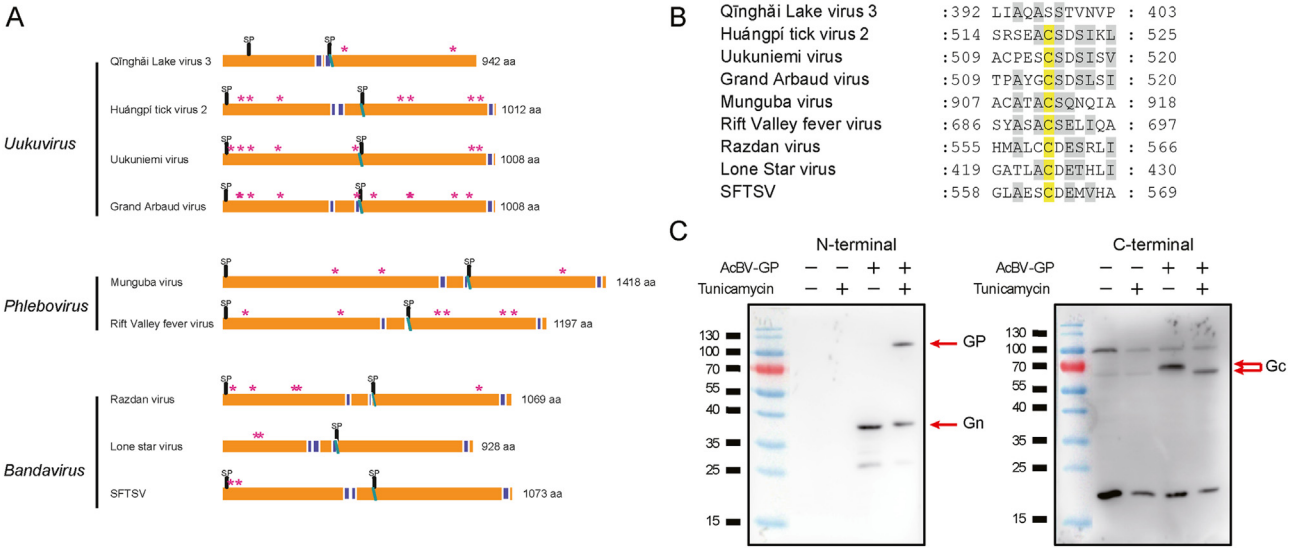

Fig. 3. Putative M segment encoding a glycoprotein with similar features to the viral glycoprotein belonging to family *Phenuiviridae*. **A** Glycoprotein features of family *Phenuiviridae*. Yellow line represents the glycoprotein, "SP" represents the signal peptide cleavage site, green slash represents the glycoprotein cleavage site, red asterisk represents the N-glycosylation site, and purple region represents the transmembrane region. **B** Alignment of glycoprotein cleavage sites. **C** Western blot result of Gn and Gc glycosylation after treatment with tunicamycin. Primary antibodies for Gn and Gc were anti-strep and anti-flag, respectively.

is removed (Fig. 3C). These results are consistent with the bioinformatics analyses, which suggest that this is a viral GP with N-glycosylation in Gc instead of Gn.

3.3. Identification of putative M segments in the QHLV3-like virus

To further validate the putative M segment of QHLV3, we used the sequence as a probe to search for M segments in other data pools from which the QHLV3 S and L segments were identified. From the RNA-seq data obtained from *Haemaphysalis sinicus*, which was collected from Qīnghǎi Province in 2023 (unpublished data), partial sequences of the S, M, and L segments (520 bp, 895 bp, and 1804 bp, respectively) with comparable abundances were found to have high identities (94%, 97%, and 99%, respectively) to QHLV3 and were designated as QHLV3 strain GC23 (Table 2). Lacking a previously reported M segment sequence, *Phenuiviridae* sp. isolate NM3GT/2021, which is phylogenetically related to QHLV3 (Fig. 2B), was identified in *Dermacentor silvarum* from Inner Mongolia in 2021 (unpublished data) (Table 2). The S and L segments of *Phenuiviridae* sp. isolate NM3GT/2021 shared 85% and 81% identity, respectively, with QHLV3. Using the probing method, we found a 528-bp sequence with 94% identity to the QHLV3 M segment (Table 2), indicating the presence of the M segment in clade 1 uukuviruses, despite it being only a partial sequence.

3.4. Epidemiological surveys of XJTAV1, QHLV1, QHLV2, and QHLV3 among the D. nuttalli tick groups

The maximum infection rates (MIRs) among tick groups indicated the prevalence of XJTAV1, QHLV1, QHLV2, and QHLV3 in *D. nuttalli* ticks from 2015 to 2017. QHLV1 had the highest MIR (49.5%) of the four tested viruses among all tick groups, with a peak (75%) detected in the tick groups of 2016. The average MIR of QHLV2 was 6.2%, with the lowest value in 2017 (2.7%) as only one group was positive. The average MIR of XJTAV1 was 8.2%, with the highest rate (31 groups) in 2015. The MIRs of QHLV3 based on L and S segments were 24.7% and 15.5%, respectively, and the rates of both segments decreased from 2015 to 2016 (Table 3). The MIR based on the M segment of QHLV3 was 21.6% and, similar to that of the L and S segments, decreased during the three years (Table 3).

In this study, the putative M segment associated with the L and S segments in tick groups was analyzed based on PCR results using the kappa test, which was performed to assess the level of agreement between MIR values. The results showed *P*-values of less than 0.05 for all three segments in the overall sample, indicating highly consistent detection results for the three segments among the tick groups. The kappa values of L and M were consistently greater than those of L and S, indicating that the association of M and L segments in the tick groups was greater than that of L and S segments (Table 4). These results further suggest that the putative M segment constitutes the QHLV3 genome.

4. Discussion

Qīnghǎi Lake is the largest saltwater lake in inland China and is an important water body for maintaining ecological security in the northeastern Qīnghǎi-Tibet Plateau. In this study, we investigated the viromes of *D. nuttalli* ticks collected around the Qīnghǎi Lake and revealed the genetic diversity of viral communities relevant to at least six viral families. Although serological evidence of CCHFV and isolation of a new subtype of TBEV have been reported in the Qīnghǎi-Tibetan Plateau area (Dai X. et al., 2018; Zhao et al., 2012), no pathogenic tick-borne viruses were found in our tick samples, perhaps because of the limited sample sizes and sampling locations. Sequences of four viruses, including three new novel viruses and one new strain of known virus, were detected at high abundance in the RNA-seq pools of ticks from 2015 to 2017, suggesting a high prevalence of these viruses among ticks.

Molecular surveys showed that the four viruses were persistently prevalent among ticks because of the high MIRs of the tick groups, implying the existence of these tick-associated viruses around Qīnghǎi Lake. These results could promote our understanding of the communities of tick-associated viruses with genetic diversity and novelty among *D. nuttalli* ticks on the Qīnghǎi-Tibetan Plateau.

D. nuttalli is primarily distributed in high-latitude regions, including Gānsù, Qīnghǎi, and Xīnjiāng in Northwest China, Hēilóngjiāng, Jílín, Liáoníng, and Inner Mongolia in Northeast China, and in the western Siberian region of Russia, Mongolia, and North Korea (Deng, 1978). So far, understanding of the viral community vectored by *D. nuttalli* ticks is limited. To our current knowledge, eight different viruses have been identified from *D. nuttalli* ticks, including Tǎchéng tick virus 1, Gùěrtú virus, TcTV2, Xīnjiāng tick associated virus 1, Xīnjiāng tick associated virus 2, and Yánggōu tick virus in Xīnjiāng, northwest China (Kholodilov et al., 2021; Li C.X. et al., 2015; Liu et al., 2020; Shen et al., 2018), Dàqìng Iflav tick virus 1 in Hēilóngjiāng, northeast China (GeneBank ON746402), and tick-borne encephalitis virus in the Russian Far East region (Kholodilov et al., 2019). Our results showed that the viruses carried by the *D. nuttalli* ticks around Qīnghǎi Lake appeared similar to those found in Xīnjiāng, a region of distinct ecologic features from

Table 2
The putative M segment sequences of QHLV3 or related to QHLV3 found in tick other pools.

Tick species	Year	Location	Strains		Length (bp)	Viral protein identity compared with QHLV3	TPM	Accession number
Dermacentor sinicus	2023	Gāngchá county	Qīnghǎi Lake virus 3 isolate GC23	L	1804	99%	0.28	OR911988
				M	895	97%	0.19	OR911989
				S	520	94%	0.15	OR911990
Dermacentor silvarum	2021	Yakxi county	*Phenuiviridae* sp. isolate NM3GT/2021	L	6665	81%	8.85	OR911985
				M	528	96%	0.17	OR911987
				S	1977	85%	3.99	OR911986

Table 3
The minimum infection rates of XJTAV1, QHLV1, QHLV2, and QHLV3 among *D. nuttalli* tick groups using nested PCR.

		2015	2016	2017	Total
		n = 31	n = 29	n = 37	n = 97
Xīnjiāng tick associated virus 1		4 (12.9%)	2 (6.9%)	2 (5.4%)	8 (8.2%)
Qīnghǎi Lake virus 1		10 (32.2%)	22 (75.9%)	16 (43.2%)	48 (49.5%)
Qīnghǎi Lake virus 2		2 (6.4%)	3 (10.3%)	1 (2.7%)	6 (6.2%)
Qīnghǎi Lake virus 3	L	13 (41.9%)	7 (24.1%)	3 (8.1%)	24 (24.7%)
	M	10 (32.2%)	7 (24.1%)	4 (10.8%)	21 (21.6%)
	S	9 (29.0%)	5 (17.2%)	1 (2.7%)	15 (15.5%)

Table 4
The results of Kappa tests with the QHLV3 prevalence based on L, M, and S segments among *D. nuttalli* tick groups.

L	M		Kappa[a]	*P*-value[b]	S		Kappa[a]	*P*-value[b]
	Positive tick groups	Negative tick groups			Positive tick groups	Negative tick groups		
2015								
Positive	8	5	0.52	0.003	6	7	0.31	0.074
Negative	2	16			3	15		
2016								
Positive	5	2	0.79	1.3×10^{-5}	6	1	0.81	1.2×10^{-5}
Negative	0	22			1	21		
2017								
Positive	2	1	0.52	0.001	0	3	−0.04	0.763
Negative	2	32			1	33		
Total								
Positive	16	7	0.65	1.6×10^{-10}	11	12	0.48	8.8×10^{-7}
Negative	5	69			4	70		

[a] The Cohen's κ-coefficient were used as a metric of interrater agreement, slight (0.0−0.20), fair (0.21−0.40), moderate (0.41−0.60), substantial (0.61−0.80), and almost perfect (0.81−1).
[b] The kappa test was used to analyze the relationship between L, S, and M segments. *P* values < 0.05 were considered statistically significant.

Qīnghǎi, but still exhibited differences. While XJTAV1 and Tǎchéng tick virus 1 were identified from both regions, the novel virus QHLV3 is closely related to TcTV2. However, the other viruses identified in *D. nuttalli* ticks from Xīnjiāng were not found in this study. Recent studies have suggested that ecological environments may play a role in shaping virome structures of specific tick species such as *H. longicornis* (Xiao et al., 2024). We speculate that the phylogenetic relationship between QHLV3 and TcTV2 may suggest a link between virus evolution and ecological adaption. Moreover, our study could provide fundamental information to characterize the potential role of the ecological environment in shaping the viromes of *D. nuttalli* ticks from Qīnghǎi Lake on the Qīnghǎi-Tibet Plateau, by further including more samples from different ecosystems. Viral communities varied among different tick species (Jia et al., 2020), and the capability to carry viruses could be associated with tick evolution (Ye et al., 2024). Due to the limited knowledge of *D. nuttalli* viromes, we did not compare the data of this study to viromes of *D. silvarum*, the tick species that is most closely related to *D. nuttalli*, although they have habitats of similar ecological features and are widely distributed in northwest and northeast China (Deng, 1978). Nevertheless, none of the reference viruses, which the novel viruses and new viral strains identified in this study were related to, are from *D. silvarum*, indicating different viral communities between *D. nuttalli* and *D. silvarum*.

Typical bunyaviruses are segmented ssRNA viruses containing L, M, and S segments. The L segment encodes the RNA-directed RNA polymerase (RdRp), which is responsible for the transcription and replication of viral genomes, the M segment encodes GP precursors that can be cleaved by host proteases into the structural GPs, Gn and Gc, and the S segment encodes the nucleocapsid protein and non-structural proteins (Guu et al., 2012). The structural protein, GP, plays a role in viral infection and assembly (Guardado-Calvo and Rey, 2017). Nucleocapsid protein wraps around the viral genome to form an RNA-protein complex (Sun et al., 2018). The non-structural protein NSs has been found to be not essential for virus growth and can be deleted, but contributes to viral pathogenesis (Eifan et al., 2013; Hedil and Kormelink, 2016). A previous study reported viromes with huge genetic diversity in diverse invertebrates (Shi et al., 2016), including a large number of novel viruses identified from ticks belonging to order *Bunyavirales*. Some of these viruses, including the Chāngpíng tick virus1, TcTV2, LITV, Bólè tick virus 1, DBTV, and YONV, constitute a new evolutionary branch closely related to genus *Phlebovirus* (Shi et al., 2016). However, almost all viruses in this new branch contain only L and S segments, with no information on the M segment (Lopez et al., 2020; Zhu et al., 2020). In 2019, TcTV2 was isolated from the serum of febrile patients in northwestern China (Dong et al., 2021). Observation of the viral particles by transmission electron microscopy suggested that TcTV-2 should contain glycoproteins. However, the M segment sequence was not detected probably due to its much lower sequence identity, which was insufficient to be identified by comparison with a known reference virus with M segment available for analysis (Dong et al., 2021). At the beginning of our study, we did not identify any M segment sequences in QHLV3 using sequence homology annotation. However, after searching unassigned sequences from the sequencing data based on length, TPM, and ORF encoded by the contigs, one contig was found to meet all the criteria, therefore exhibiting the potential to be the M segment of QHLV3. This putative M segment encodes a GP with features similar to those of other uukuviruses, phleboviruses, and bandaviruses, which was confirmed with N-glycosylation and could be cleaved into Gn and Gc. We attempted to construct the 3D structure of this putative GP using AlphaFold2, together with the GPs of other uukuviruses and phleboviruses as controls. However, probably because of the extremely low sequence identities between QHLV3 and other viruses (Supplementary Fig. S4), the structure of this protein differed greatly from that of the other viral proteins (data not shown). Moreover, the MIR detection results showed no significant differences in the MIRs of the three segments in each tick group. This suggests that, although the sensitivities of the methods used to detect the three segments might differ, detection of the L, M, and S segments was consistent among the tick groups. Following the same method, the M segment was also identified in other tick samples (Table 2). During subsequent surveys following this study, we identified the sequences of a new strain of QHLV3 from one group of tick samples collected from Qīnghǎi Lake in 2023. Although these sequences were partial sequences of the L, M, and S segments, they demonstrated the persistent presence of QHLV3 containing three segments in ticks in Qīnghǎi, even after six years. Furthermore, identification of the M segment sequence from a tick pool from Inner Mongolia, in which L and S segments of the *Phenuiviridae* sp. isolate NM3GT/2021 were found, also suggested the presence of the M segment in viruses close to QHLV3. Therefore, our results suggest the existence of the M segment in the novel virus QHLV3; this also indicates the presence of the M segment in viruses of genus *Uukuvirus* clade I, which may not be identified because of its high diversity.

This study has limitations. First, only *D. nuttalli* tick samples were collected around Qīnghǎi Lake, the data of which may not present the overall viral structure of this tick species in the Qīnghǎi-Tibet Plateau. Second, owing to the limited sample size, viral isolation was not conducted in this study; thus, the infectivity and pathogenicity of newly discovered viruses remain unclear. Third, because the surveys in this study were performed among tick groups before our previous study (Zhang et al., 2021), which established a virus detection method in tick individuals, the results did not reveal a precise prevalence rate of viruses in ticks. Nevertheless, statistical analysis still suggested the relevance of the QHLV3 L, M, and S segments detected in the tick groups. Moreover, as TcTV-2 has been recently identified as a causative agent of human febrile disease (Dong et al., 2021), we speculate that QHLV3 may also pose a risk of infection to humans and animals. However, due to the lack of serum

samples, we were unable to evaluate the risk of exposure to QHLV3 in human and animal hosts.

5. Conclusions

In this study, we characterized the viromes of *Dermacentor nuttalli* in Qīnghǎi Province from 2015 to 2017. The results revealed viral sequences associated with at least six families, including the identification of four novel RNA viruses, which enhances our understanding of the viromes of *D. nuttalli* ticks in highland regions. One of these viruses belongs to an unassigned group in the genus *Uukuvirus* of the family *Phenuiviridae* and order *Bunyavirales* (referred to as Qīnghǎi Lake virus 3, QHLV3), whereas the others remain unclassified. Notably, a putative M segment of QHLV3 was discovered in the sequencing data, which was absent in other clade I uukuviruses. These findings highlight the importance of an M segment encoding the structural glycoprotein when constructing segmented bunyaviruses, and provide valuable insights into the discovery of novel viruses from ticks.

Data availability

The datasets generated and analyzed in this study have been deposited in the GenBank Sequence Read Archive (SRA) under the accession number PRJNA1043875 and ScienceDB (https://doi.org/10.57760/sciencedb.18146). Viral sequences identified in this study were deposited in Genebank under accession number OR837771–3 and OR911985–93.

Ethics statement

This article does not contain any studies with human or animal subjects performed by any of the authors.

Author contributions

Yaohui Fang: data curation, formal analysis, investigation, methodology, software, writing-original draft. Jun Wang: data curation, formal analysis, software. Jianqing Sun: resource, investigation. Zhengyuan Su: resource, data curation, formal analysis, investigation, methodology. Shengyao Chen: investigation, methodology. Jian Xiao: data curation, formal analysis, software. Jun Ni: data curation, formal analysis, software. Zhihong Hu: funding acquisition, project administration, supervision, validation. Yubang He: resource, investigation, project administration, supervision, validation. Shu Shen: data curation, formal analysis, investigation, conceptualization, funding acquisition, project administration, supervision, validation, writing-review & editing. Fei Deng: conceptualization, funding acquisition, project administration, supervision, validation, writing-review & editing.

Conflict of interest

Prof. Fei Deng is an editorial board member for *Virologica Sinica* and was not involved in the editorial review or the decision to publish this article. The authors declare that they have no conflict of interest.

Acknowledgements

We would like to thank Dr. Zhixian Qiao and Xiaocui Chai at the Analysis and Testing Center of the Institute of Hydrobiology, Chinese Academy of Sciences, for their assistance with RNA-seq and data analysis. This study was supported by the National Key R&D Program of China (2022YFC2305100, 2021YFC2300900), the Key Deployment Projects of the Chinese Academy of Sciences (KJZD-SW-L11), the Youth Project of the Wuhan Institute of Virology, Chinese Academy of Sciences (2023QNTJ-03), the Biological Resources Program, Chinese Academy of Sciences (KFJ-BRP-017-74), and the National Basic Science Data Sharing Service Platform (NBSDC-DB-13).

Appendix A. Supplementary data

Supplementary data to this article can be found online at https://doi.org/10.1016/j.virs.2024.04.006.

References

Ambrose, R.L., Lander, G.C., Maaty, W.S., Bothner, B., Johnson, J.E., Johnson, K.N., 2009. Drosophila A virus is an unusual RNA virus with a T=3 icosahedral core and permuted RNA-dependent RNA polymerase. J. Gen. Virol. 90, 2191–2200.
Bolger, A.M., Lohse, M., Usadel, B., 2014. Trimmomatic: a flexible trimmer for Illumina sequence data. Bioinformatics 30, 2114–2120.
Boulanger, N., Boyer, P., Talagrand-Reboul, E., Hansmann, Y., 2019. Ticks and tick-borne diseases. Med. Maladies Infect. 49, 87–97.
Chitimia, L., Lin, R.Q., Cosoroaba, I., Braila, P., Song, H.Q., Zhu, X.Q., 2009. Molecular characterization of hard and soft ticks from Romania by sequences of the internal transcribed spacers of ribosomal DNA. Parasitol. Res. 105, 907–911.
Dai, S., Zhang, T., Zhang, Y., Wang, H., Deng, F., 2018. Zika virus baculovirus-expressed virus-like particles induce neutralizing antibodies in mice. Virol. Sin. 33, 213–226.
Dai, X., Shang, G., Lu, S., Yang, J., Xu, J., 2018. A new subtype of eastern tick-borne encephalitis virus discovered in Qinghai-Tibet Plateau, China. Emerg. Microb. Infect. 7, 74.
Deng, G., 1978. Economic Insect Fauna of China. Science Press.
Dong, Z., Yang, M., Wang, Z., Zhao, Shuo, Xie, S., Yang, Y., Liu, G., Zhao, Shanshan, Xie, J., Liu, Q., Wang, Y., 2021. Human tacheng tick virus 2 infection, China, 2019. Emerg. Infect. Dis. 27, 594–598.
Eifan, S., Schnettler, E., Dietrich, I., Kohl, A., Blomström, A.-L., 2013. Non-structural proteins of arthropod-borne bunyaviruses: roles and functions. Viruses 5, 2447–2468.
Geng, Z., Hou, X.X., Wan, K.L., Hao, Q., 2010. [Isolation and identification of Borrelia burgdorferi sensu lato from ticks in six provinces in China]. Zhonghua Liuxingbingxue Zazhi 31, 1346–1348.
Grabherr, M.G., Haas, B.J., Yassour, M., Levin, J.Z., Thompson, D.A., Amit, I., Adiconis, X., Fan, L., Raychowdhury, R., Zeng, Q., Chen, Z., Mauceli, E., Hacohen, N., Gnirke, A., Rhind, N., di Palma, F., Birren, B.W., Nusbaum, C., Lindblad-Toh, K., Friedman, N., Regev, A., 2011. Full-length transcriptome assembly from RNA-Seq data without a reference genome. Nat. Biotechnol. 29, 644–652.
Guardado-Calvo, P., Rey, F.A., 2017. The envelope proteins of the Bunyavirales. Adv. Virus Res. 98 (98), 83–118.
Guu, T.S.Y., Zheng, W., Tao, Y.J., 2012. Bunyavirus: structure and replication. Adv. Exp. Med. Biol. 726, 245–266.
Han, R., Yang, J., Niu, Q., Liu, Z., Chen, Z., Kan, W., Hu, G., Liu, G., Luo, J., Yin, H., 2018. Molecular prevalence of spotted fever group rickettsiae in ticks from Qinghai Province, northwestern China. Infect. Genet. Evol. 57, 1–7.
Hedil, M., Kormelink, R., 2016. Viral RNA silencing suppression: the enigma of bunyavirus NSs proteins. Viruses 8, 208.
Huson, D.H., Auch, A.F., Qi, J., Schuster, S.C., 2007. MEGAN analysis of metagenomic data. Genome Res. 17, 377–386.
Jia, N., Wang, J., Shi, W., Du, L., Sun, Y., Zhan, W., Jiang, J.F., Wang, Q., Zhang, B., Ji, P., Bell-Sakyi, L., Cui, X.M., Yuan, T.T., Jiang, B.G., Yang, W.F., Lam, T.T.Y., Chang, Q.C., Ding, S.J., Wang, X.J., Zhu, J.G., et al., 2020. Large-scale comparative analyses of tick genomes elucidate their genetic diversity and vector capacities. Cell 182, 1328–1340.e13.
Kholodilov, I., Belova, O., Burenkova, L., Korotkov, Y., Romanova, L., Morozova, L., Kudriavtsev, V., Gmyl, L., Belyaletdinova, I., Chumakov, A., Chumakova, N., Dargyn, O., Galatsevich, N., Gmyl, A., Mikhailov, M., Oorzhak, N., Polienko, A., Saryglar, A., Volok, V., Yakovlev, A., Karganova, G., 2019. Ixodid ticks and tick-borne encephalitis virus prevalence in the South Asian part of Russia (Republic of Tuva). Ticks and Tick-borne Dis. 10, 959–969.
Kholodilov, I.S., Belova, O.A., Morozkin, E.S., Litov, A.G., Ivannikova, A.Y., Makenov, M.T., Shchetinin, A.M., Aibulatov, S.V., Bazarova, G.K., Bell-Sakyi, L., et al., 2021. Geographical and tick-dependent distribution of flavi-like alongshan and yanggou tick viruses in Russia. Viruses 13, 458.
Kuhn, J.H., Abe, J., Adkins, S., Alkhovsky, S.V., Avšič-Županc, T., Ayllón, M.A., Bahl, J., Balkema-Buschmann, A., Ballinger, M.J., Kumar Baranwal, V., et al., 2023. Annual (2023) taxonomic update of RNA-directed RNA polymerase-encoding negative-sense RNA viruses (realm Riboviria: kingdom Orthornavirae: phylum Negarnaviricota). J. Gen. Virol. 104, 001864.
Langmead, B., Salzberg, S.L., 2012. Fast gapped-read alignment with Bowtie 2. Nat. Methods 9, 357–359.
Li, C.X., Shi, M., Tian, J.H., Lin, X.D., Kang, Y.J., Chen, L.J., Qin, X.C., Xu, J., Holmes, E.C., Zhang, Y.Z., 2015. Unprecedented genomic diversity of RNA viruses in arthropods reveals the ancestry of negative-sense RNA viruses. Elife 4, e05378.
Li, Y., Liu, P., Wang, C., Chen, G., Kang, M., Liu, D., Li, Z., He, H., Dong, Y., Zhang, Y., 2015. Serologic evidence for Babesia bigemina infection in wild yak (Bos mutus) in Qinghai province, China. J. Wildl. Dis. 51, 872–875.
Liu, X., Zhang, X., Wang, Z., Dong, Z., Xie, S., Jiang, M., Song, R., Ma, J., Chen, S., Chen, K., Zhang, H., Si, X., Li, C., Jin, N., Wang, Y., Liu, Q., 2020. A tentative tamdy orthonairovirus related to febrile illness in northwestern China. Clin. Infect. Dis. 70, 2155–2160.
Lopez, Y., Miranda, J., Mattar, S., Gonzalez, M., Rovnak, J., 2020. First report of lihan tick virus (phlebovirus, Phenuiviridae) in ticks, Colombia. Virol. J. 17, 63.
Lu, X., Lin, X.D., Wang, J.B., Qin, X.C., Tian, J.H., Guo, W.P., Fan, F.N., Shao, R., Xu, J., Zhang, Y.Z., 2013. Molecular survey of hard ticks in endemic areas of tick-borne diseases in China. Ticks Tick Borne Dis. 4, 288–296.

Shen, S., Duan, X., Wang, B., Zhu, L., Zhang, Y., Zhang, J., Wang, J., Luo, T., Kou, C., Liu, D., Lv, C., Zhang, L., Chang, C., Su, Z., Tang, S., Qiao, J., Moming, A., Wang, C., Abudurexiti, A., Wang, H., Hu, Z., Zhang, Y., Sun, S., Deng, F., 2018. A novel tick-borne phlebovirus, closely related to severe fever with thrombocytopenia syndrome virus and Heartland virus, is a potential pathogen. Emerg. Microb. Infect. 7, 95.

Shi, M., Lin, X.D., Tian, J.H., Chen, L.J., Chen, X., Li, C.X., Qin, X.C., Li, J., Cao, J.P., Eden, J.S., Buchmann, J., Wang, W., Xu, J., Holmes, E.C., Zhang, Y.Z., 2016. Redefining the invertebrate RNA virosphere. Nature 540, 539–543.

Sun, Y., Li, J., Gao, G.F., Tien, P., Liu, W., 2018. Bunyavirales ribonucleoproteins: the viral replication and transcription machinery. Crit. Rev. Microbiol. 44, 522–540.

Tamura, K., Stecher, G., Peterson, D., Filipski, A., Kumar, S., 2013. MEGA6: molecular evolutionary genetics analysis version 6.0. Mol. Biol. Evol. 30, 2725–2729.

Tokarz, R., Williams, S.H., Sameroff, S., Sanchez Leon, M., Jain, K., Lipkin, W.I., 2014. Virome analysis of Amblyomma americanum, Dermacentor variabilis, and Ixodes scapularis ticks reveals novel highly divergent vertebrate and invertebrate viruses. J. Virol. 88, 11480–11492.

Xia, Y., 2020. Correlation and association analyses in microbiome study integrating multiomics in health and disease. Prog. Mol. Biol. Transl. Sci. 171, 309–491.

Xiao, J., Yao, X., Guan, X., Xiong, J., Fang, Y., Zhang, J., Zhang, Y., Moming, A., Su, Z., Jin, J., Ge, Y., Wang, J., Fan, Z., Tang, S., Shen, S., Deng, F., 2024. Viromes of Haemaphysalis longicornis reveal different viral abundance and diversity in free and engorged ticks. Virol. Sin. 39, 194–204.

Yang, Y., Diwu, J., Cao, J., Zhang, Jijun, Luo, X., Gao, X., Qiang, L.I., Zhang, Junmin, 2008. Investigation on kinds and nature geographic distribution of ticks in Qinghai province. Chin. J. Hyg. Insect. Equip. 14, 201–203.

Ye, R.Z., Li, Y.Y., Xu, D.L., Wang, B.H., Wang, X.Y., Zhang, M.Z., Wang, N., Gao, W.Y., Li, C., Han, X.Y., Du, L.F., Xia, L.Y., Song, K., Xu, Q., Liu, J., Cheng, N., Li, Z.H., Du, Y.D., Yu, H.J., Shi, X.Y., Jiang, J.F., Sun, Y., , Tick Genome and Microbiome Consortium (TIGMIC), Cui, X.M., Ding, S.J., Zhao, L., Cao, W.C., 2024. Virome diversity shaped by genetic evolution and ecological landscape of Haemaphysalis longicornis. Microbiome 12, 35.

Yin, H., Luo, J., Schnittger, L., Lu, B., Beyer, D., Ma, M., Guan, G., Bai, Q., Lu, C., Ahmed, J., 2004. Phylogenetic analysis of Theileria species transmitted by Haemaphysalis qinghaiensis. Parasitol. Res. 92, 36–42.

Yu, Z., Wang, H., Wang, T., Sun, W., Yang, X., Liu, J., 2015. Tick-borne pathogens and the vector potential of ticks in China. Parasites Vectors 8, 24.

Zhang, Y., Hu, B., Agwanda, B., Fang, Y., Wang, J., Kuria, S., Yang, J., Masika, M., Tang, S., Lichoti, J., Fan, Z., Shi, Z., Ommeh, S., Wang, H., Deng, F., Shen, S., 2021. Viromes and surveys of RNA viruses in camel-derived ticks revealing transmission patterns of novel tick-borne viral pathogens in Kenya. Emerg. Microb. Infect. 10, 1975–1987.

Zhao, J., Wang, H., Wang, Y., 2012. Regional distribution profiles of tick-borne pathogens in China. Chin. J. Vector Biol. Control 23, 445–448.

Zhao, Y., Li, M.C., Konaté, M.M., Chen, L., Das, B., Karlovich, C., Williams, P.M., Evrard, Y.A., Doroshow, J.H., McShane, L.M., 2021. TPM, FPKM, or normalized counts? A comparative study of quantification measures for the analysis of RNA-seq data from the NCI patient-derived models repository. J. Transl. Med. 19, 269.

Zhu, C.Q., He, T., Wu, T., Ai, L.L., Hu, D., Yang, X.H., Lv, R.C., Yang, L., Lv, H., Tan, W.L., 2020. Distribution and phylogenetic analysis of Dabieshan tick virus in ticks collected from Zhoushan, China. J. Vet. Med. Sci. 82, 1226–1230.